

# TENSILE PROPERTIES OF GEOGRIDS UNDER CYCLIC LOADINGS

By Hoe I. Ling,<sup>1</sup> Yoshiyuki Mohri,<sup>2</sup> and Toshinori Kawabata,<sup>3</sup> Members, ASCE

**ABSTRACT:** The tensile behavior of three commonly used polymeric geogrids (polypropylene, polyester, and high-density polyethylene) under cyclic loading was investigated. The tests were strain controlled and were conducted for 100 cycles at different load ratios. The stiffness and damping ratio of geogrids at all load cycles were compared with the primary loading curve. The stiffness increased while the damping ratio decreased with more loading cycles at any load ratio. A higher load ratio decreased the stiffness ratio and increased the damping ratio. The strengths of prestressed and virgin specimens were also compared. Negligible strength reduction resulted from short-term cyclic loading. The strength obtained from static tests appears reasonable when used for design considering short-term cyclic loading. An empirical relationship is proposed to determine the strain accumulated from cyclic loading under different load ratios.

## INTRODUCTION

Geosynthetics are used as tensile reinforcement in many applications, both on land and underwater (e.g., Koerner 1998). They are subject not only to sustained tensile load but also to repeated load such as that generated by traffic, water waves, and earthquakes. The tensile properties of geosynthetic reinforcements under static loading have been a topic of major research over the past few decades, and the testing procedure has been standardized (e.g., ASTM D 4632, ASTM D 4595, GRI GG1).

Very limited studies have, however, been conducted to investigate the tensile properties of geosynthetics under cyclic loadings. Bathurst and Cai (1994) presented results of polyester (PET) and high-density polyethylene (HDPE) geogrids tested under different load amplitudes and frequencies, ranging from 0.1 to 3.5 Hz, each for a total of 10 cycles. They concluded that the tensile properties of HDPE geogrid were sensitive to loading frequencies but the polyester geogrids were not. The results showed that the area of hysteresis loop increases as the load level increases. HDPE showed reduced stiffness with the load levels, whereas PET showed a reduction followed by an increase.

Moraci and Montanelli (1996, 1997) also conducted cyclic loading tests on PET and HDPE geogrids. Their tests were conducted for different frequencies (0.1 to 1 Hz) and up to 10,000 cycles. The results showed that stiffness increases and damping reduces with more load cycles, which is in agreement with the trend of results reported by Bathurst and Cai (1994). Both Bathurst and Cai (1994) and Moraci and Montanelli (1996, 1997) used a load amplitude of 20%, 40%, 60%, and 80% of the strength obtained from monotonic loading test. Ashmawy and Bourdeau (1996) tested nonwoven polypropylene and woven polyester geotextiles. Their test results showed a higher permanent strain for geotextiles manufactured from polypropylene when compared to that of polyester.

This study focused on the loads induced in geosynthetic reinforcement for relatively short duration, such as those generated by an earthquake. A series of cyclic tension tests were conducted on three types of geogrid using a constant strain

rate. The cyclic tensile properties, such as stiffness, damping ratio, and strength, are presented and discussed. A simple equation is proposed to relate strain with cycles of loading and load ratios.

## MATERIAL AND TEST CONDITIONS

Three types of geogrid (denoted A, B, and C), of rather similar strength but different polymer types, were used in this study: Geogrids A, B, and C were manufactured from polypropylene (PP), PET, and HDPE, respectively. Geogrid A is a biaxial grid, whereas geogrids B and C are uniaxial grids. Their index properties are given in Table 1. The strength of these materials was 50–60% smaller than those used by Bathurst and Cai (1994) or Moraci and Montanelli (1996, 1997).

Single-rib geogrid specimens were prepared from a roll of each geosynthetic sample. The gage length of geogrids A, B, and C are 22, 33, and 33 cm, respectively (number of apertures: 7, 12, 2). The single-rib specimen was used because it fit the clamping jaws of the available device. The nodes of geogrids A and C allowed them to be clamped to the jaws of a loading device. Geogrid B was smooth, and therefore its two ends were stiffened with epoxy and clamped to the jaw to prevent slippage. Note that the selected dimensions satisfied GRI GG1 Standard, which calls for a specimen having at least two apertures or a specimen 22 cm long. The test result obtained from a single-rib geogrid was multiplied by the total ribs in a meter width to give the load per unit width. Note that a wide-width test (ASTM D 4595) is recommended if the results are to be used for design.

The specimens were tested along their machine direction under a constant strain rate of 10% per minute, in accordance with the rate specified by ASTM D 4595. For each type of geogrid, a monotonic and five cyclic tests were conducted. The cyclic tests were conducted under 10%, 20%, 40%, 60%, and 80% of the peak strength obtained from respective monotonic tests. A total of 100 cycles were conducted for each cyclic test with the same strain rate (10% per minute) for both loading and unloading. After the cyclic test, the specimen was again loaded monotonically to failure. All tests were conducted in a temperature-controlled room at 20° C.

## RESULTS AND DISCUSSION

Fig. 1(a)–(c) shows the results of monotonic and cyclic loading tests. The strengths obtained from monotonic tests are summarized in Table 1; they were used as reference values for subsequent cyclic loading tests. The shape of the monotonic loading curve of geogrid B is typical of knitted polyester geogrids. It ruptured abruptly when the peak strength was reached. The difference in the properties of geogrids A, B, and C are likely due to the polymer properties and manufacturing process. PP and HDPE are in their elastic/plastic state at ambient

<sup>1</sup>Asst. Prof., Dept. of Civ. and Envir. Engrg., Univ. of Delaware, Newark, DE 19716.

<sup>2</sup>Res. Mgr., Lab. of Soil Engrg., Nat. Res. Inst. of Ag. Engrg., 2-1-2 Kannodai, Tsukuba 305, Japan.

<sup>3</sup>Res. Mgr., Pipe Engrg. Dept., Kubota Corp., 3-1-3 Nihonbashi-Muromachi, Chuo-ku, Tokyo, 103, Japan.

Note. Discussion open until January 1, 1999. To extend the closing date one month, a written request must be filed with the ASCE Manager of Journals. The manuscript for this technical note was submitted for review and possible publication on September 11, 1997. This technical note is part of the *Journal of Geotechnical and Geoenvironmental Engineering*, Vol. 124, No. 8, August, 1998. ©ASCE, ISSN 1090-0241/98/0008-0782-0787/\$8.00 + \$.50 per page. Technical Note No. 16582.

**TABLE 1. Index Properties of Geogrids**

Geogrid (1)	Polymer type (2)	Manufacturing process (3)	Aperture Size		Mass per unit area (g/m <sup>2</sup> ) (6)	Tensile strength (kN/m) (7)	Glass transition temperature (°C) (8)
			Machine direction (cm) (4)	Cross-machine direction (cm) (5)			
A	Polypropylene	Punched sheet drawn	2.8	3.3	550	46	75-80
B	Polyester	Punched sheet drawn	2.03	2.54	187	46	-10
C	High-density polyethylene	Woven	14.5	1.7	510	54	-80

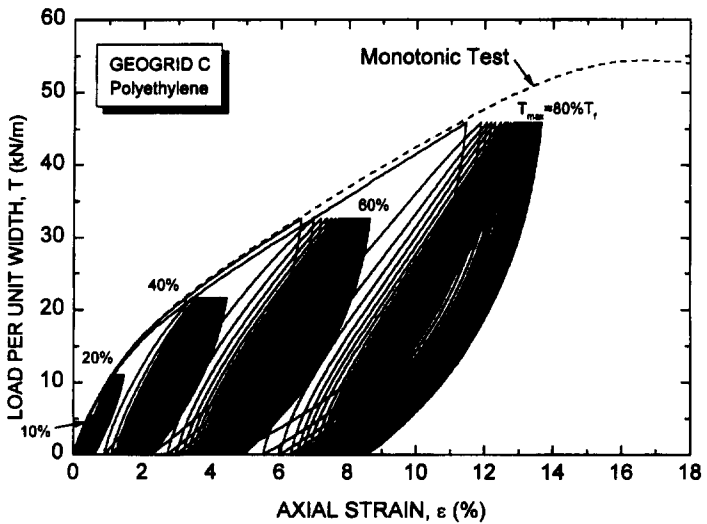
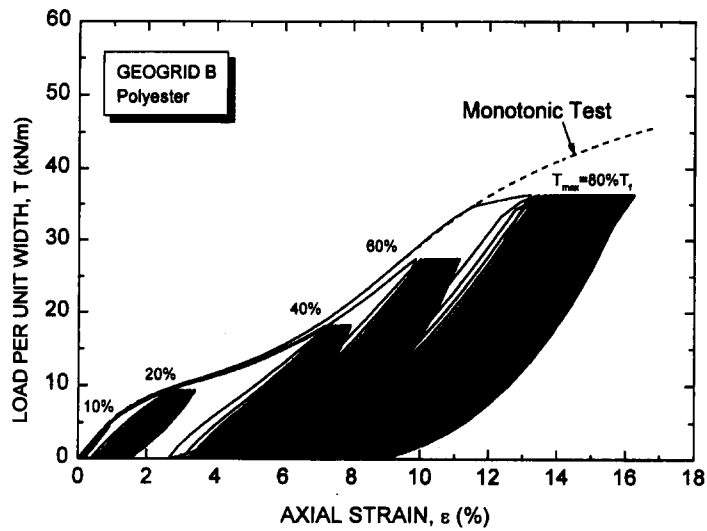
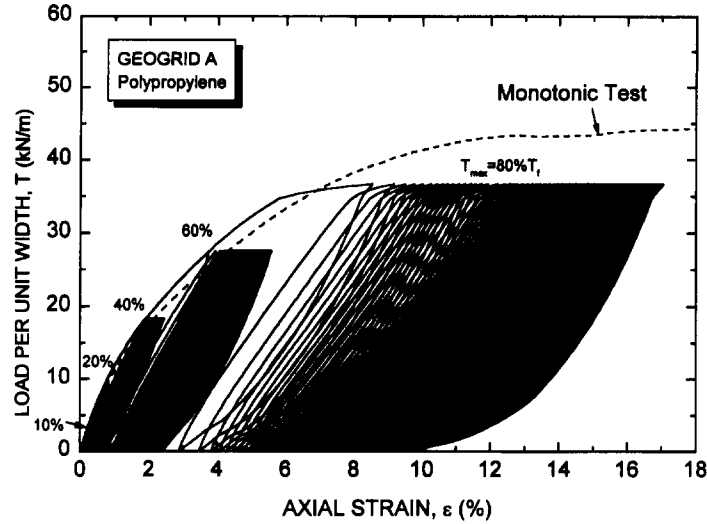


**FIG. 1. Load-Strain Relationships of Monotonic and Cyclic Loading: (a) Geogrid A; (b) Geogrid B; (c) Geogrid C**

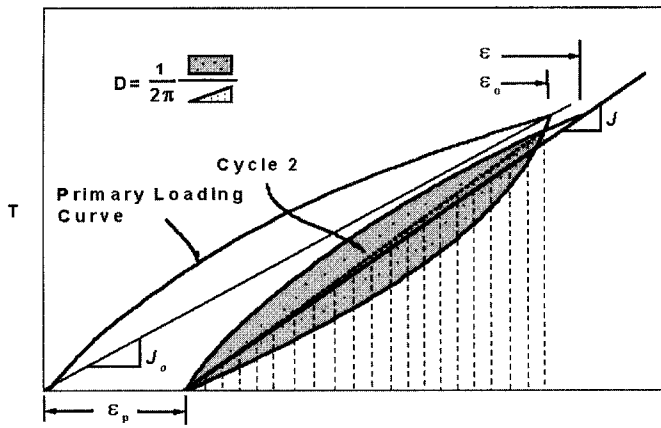


FIG. 2. Definition of Stiffness and Damping Ratio

temperature. PET is in its glassy state and, therefore, stiff and more brittle (see Table 1 for glass transition temperatures). The shape of the stress-strain curve of geogrid B is due to the manufacturing process. It is a woven, coated product. At low stress levels, it undergoes relatively large strain to take out the slack from the manufacturing. On the other hand, geogrids A and C are manufactured by punching and drawing sheets of material.

The primary loading curve obtained in cyclic tests showed that there were very few variations in the properties of the specimens. It also showed that the stiffness of the primary loading curve was less than that of subsequent load cycles. All the specimens survived 100 cycles of loading up to a maximum load ratio  $R_T = 80\%$ , except geogrid B, which ruptured during the 64th load cycle (at  $R_T = 80\%$ ). The strain in the geogrid accumulated with loading cycles, and the rate of accumulation became greater with increasing load ratio. The unloading and reloading curves described a larger loop when  $R_T$  increased. For a small value of  $R_T$ , such as 10%, the loop described by the unloading-reloading curves was very small and close to linear. Because the tests were strain controlled, the time taken to complete a loop at high load amplitude was naturally more than that conducted at a low load amplitude. Typical frequencies of cyclic tests were 0.25 and 0.02 Hz at  $R_T = 10\%$  and 80%, respectively.

The stiffness,  $J$ , of the reloading curve in each load cycle was normalized by the stiffness of the primary loading curve  $J_0$  to give a stiffness ratio (Fig. 2). Fig. 3(a) shows the variation of stiffness ratio of the geogrids with different load cycles and load ratios. The results show that at a small load ratio, say  $R_T = 10\%$ , the stiffness was not significantly affected by the cycles of loading. At higher  $R_T$ , the stiffness increased with load cycles. For geogrid C, the stiffness tended to increase for all levels of load ratio. For geogrid A, at  $R_T = 80\%$ , the stiffness started to decrease after 10 loading cycles.

The energy dissipated in each load cycle,  $\Delta W$ , is normalized by the elastic strain energy,  $W$ , to give the damping ratio  $D$  (Fig. 2):

$$D = \frac{1}{2\pi} \frac{\Delta W}{W} \quad (1)$$

As shown in Fig. 3(b), the damping ratio increases with an increase in load ratio. A reduction in damping ratio with loading cycles occurred for all three types of geogrid at different load ratios. For geogrid B, the energy loss was also proportional to load ratios. However, because of the shape of the load-strain curve, which is S-shaped, the damping ratio calculated at 20% to 80% load ratios was reversed.

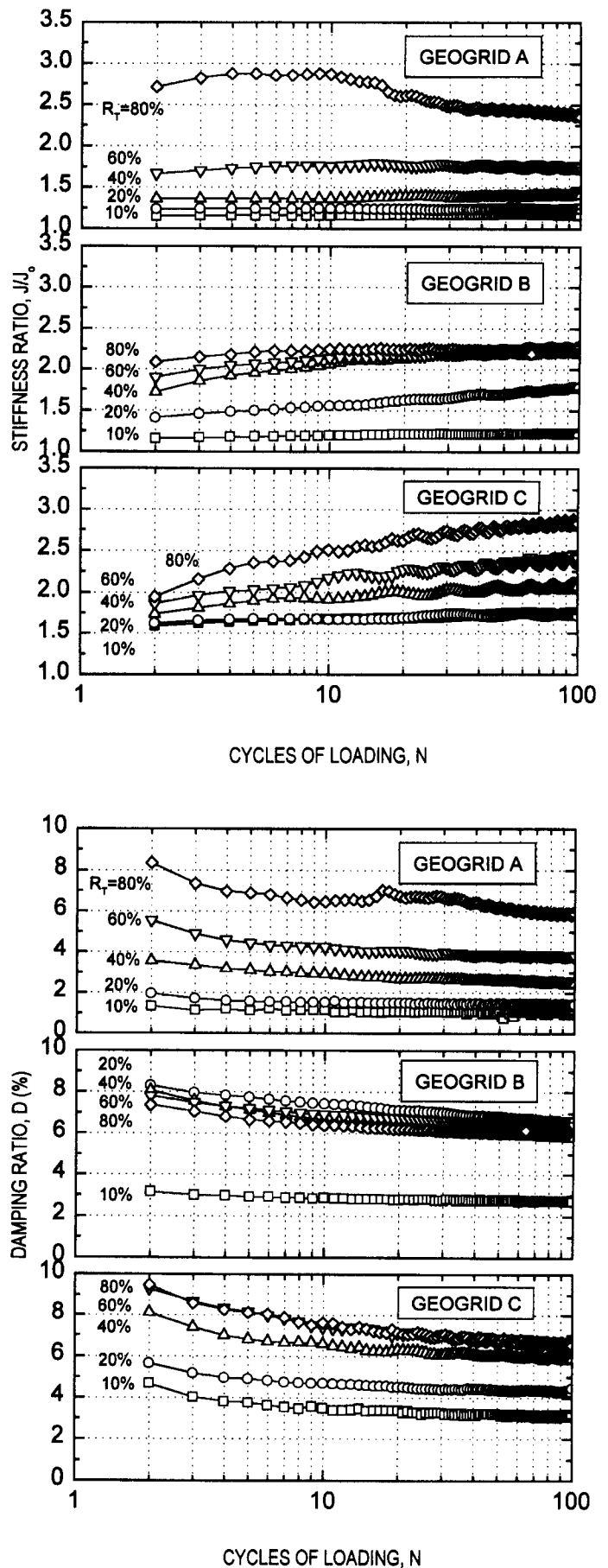


FIG. 3. (a) Relationships between Stiffness Ratio and Load Cycles; (b) Relationships between Damping Ratio and Load Cycles

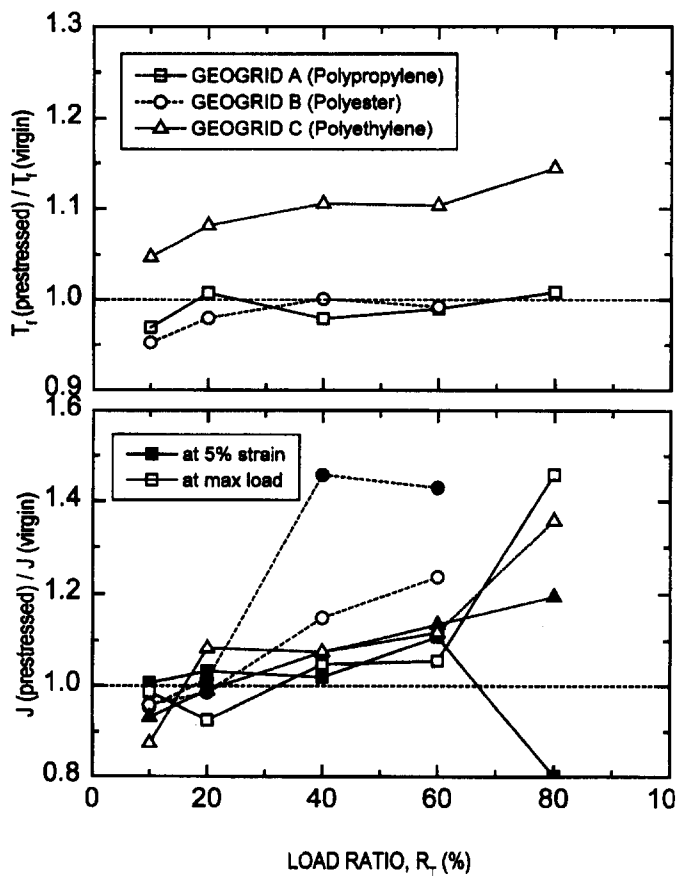
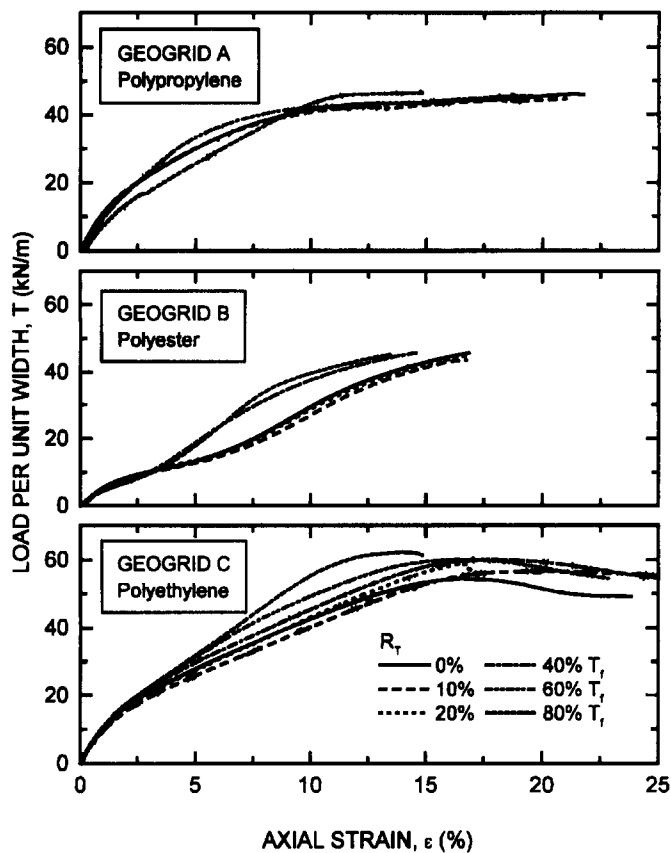
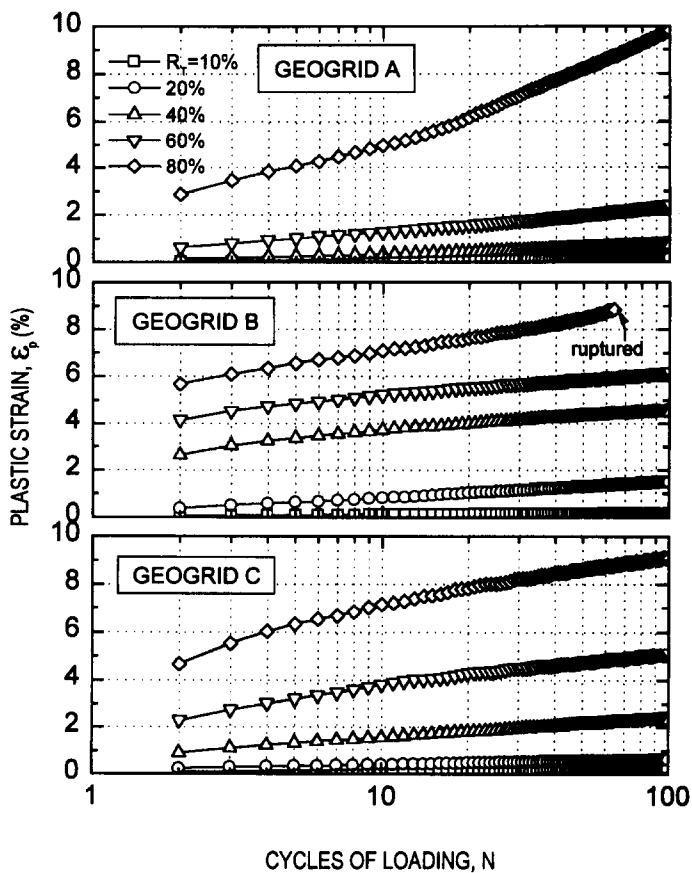
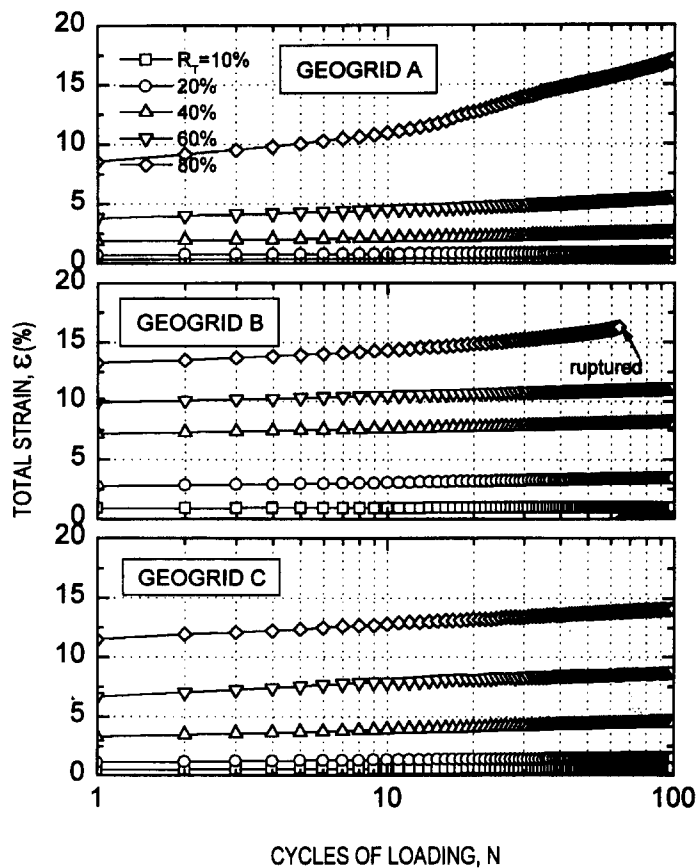


FIG. 4. (a) Relationships between Total Strain and Load Cycles; (b) Relationships between Plastic Strain and Load Cycles

FIG. 5. Virgin and Prestressed Specimens: (a) Load-Strain Relationships; (b) Strength and Stiffness Ratios

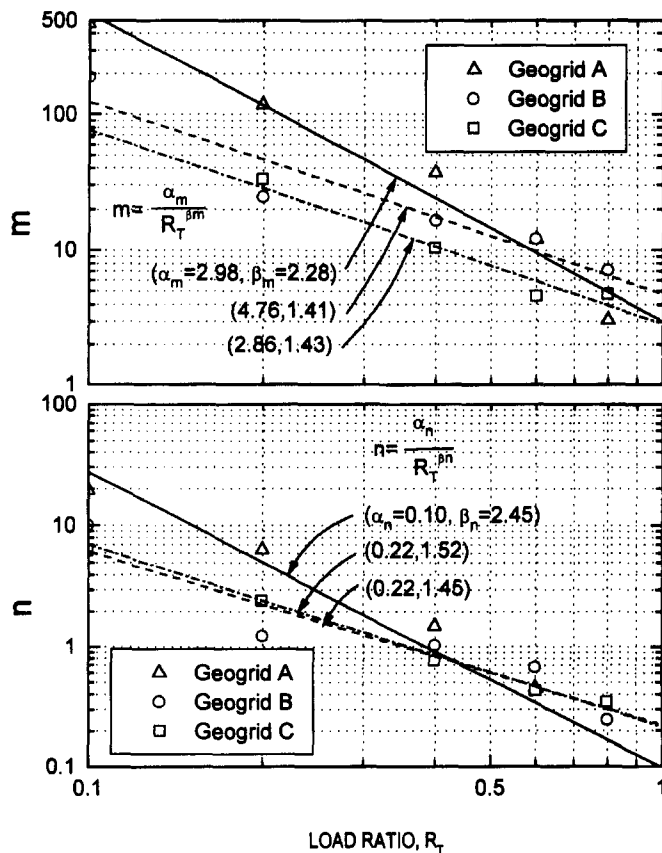
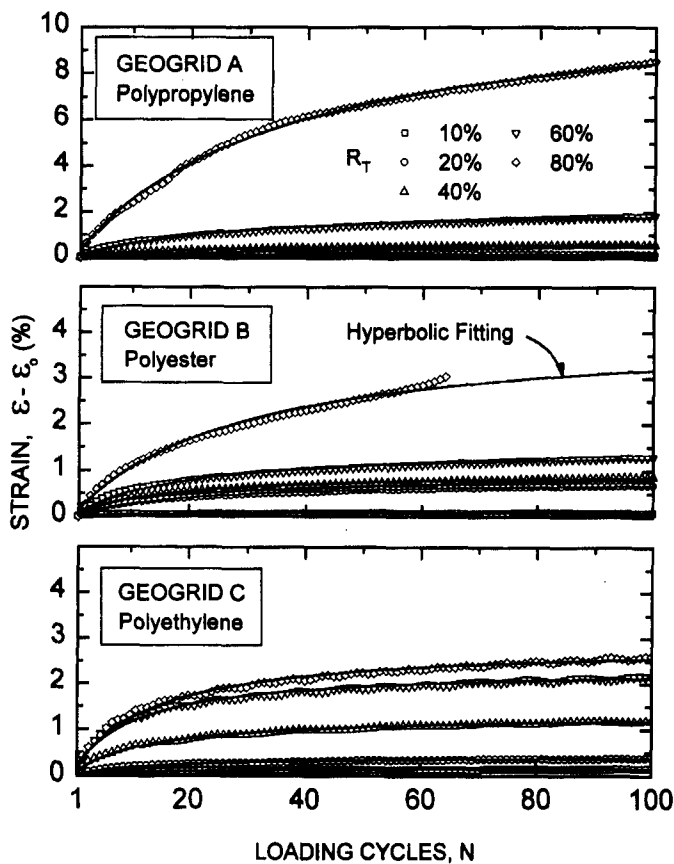


FIG. 6. (a) Strain Induced by Load Cycles and Hyperbolic Approximation; (b)  $m$  and  $n$  versus Load Ratio Relationships

The total strain and plastic strain ( $\epsilon$  and  $\epsilon_p$ , see Fig. 2) of the geogrids for all loading cycles are shown in Figs. 4(a) and (b), respectively. The results indicate that both plastic and total strains accumulate with cycles of loading. At large load ratios, strains accumulate rapidly with cyclic loading. The total strain developed after 100 loading cycles ranged from 0.3% at  $R_T = 10\%$  to 20% at  $R_T = 80\%$ . Note that for geogrid B, the specimen tested at  $R_T = 80\%$  ruptured during cyclic loading; and this has been confirmed with additional testing.

To investigate the effects of prestressing on geogrids, the specimens were loaded monotonically to failure after cyclic loading test. Fig. 5(a) compares the results of virgin and prestressed specimens. The effect of prestressing seems negligibly small for geogrid A. For geogrids B and C, relationships were not affected much by prestressing at low load ratio, but a higher stiffness and strength resulted when  $R_T$  was above 40%. The failure strain reduced with prestressing. The ratios of the strength of prestressed and virgin specimens are summarized in Fig. 5(b). There were no significant degradations of strength by prestressing. The stiffness of prestressed specimens, at 5% strain and at failure, increased with the load ratio.

The strain accumulated from load cycles may be used to estimate the elongation of geosynthetic reinforcement and thus deformation of the structure, such as the reinforced soil structures. The relationships between strain accumulated from cyclic loading  $\epsilon - \epsilon_0$  and load cycles  $N$  are expressed using a hyperbolic relationship (Fig. 6[a]):

$$\epsilon - \epsilon_0 = \frac{N}{m + n \cdot N} \quad (2)$$

where  $\epsilon_0$  is the strain developed during primary loading and  $m$  and  $n$  are constants. A correlation coefficient close to unity was obtained for the relationship at all load ratios. A hyperbolic relationship gave a more reasonable simulation of strain accumulated by cyclic loading than the linear  $\epsilon$  versus  $\log N$  relationship used by Moraci and Montanelli (1997). The curve is not linear in the  $\epsilon - \log N$  plotting, especially at a high load ratio (Fig. 4[a]).

The constants ( $m$  and  $n$ ) may be correlated to load ratios  $R_T$  through a power law (Fig. 6[b]):

$$m = \frac{\alpha_m}{R_T^{\beta_m}} \quad (3)$$

$$n = \frac{\alpha_n}{R_T^{\beta_n}} \quad (4)$$

where  $\alpha_m$ ,  $\alpha_n$ ,  $\beta_m$ , and  $\beta_n$  are parameters. The values of these parameters are shown in Fig. 6(b) for the three types of geogrid.

## CONCLUSIONS

A series of monotonic and cyclic loading tests were conducted on three major types of geogrid manufactured from polypropylene, polyester, and high-density polyethylene. The results showed that the strength of polypropylene geogrid was not affected significantly by cyclic loading. The strength of polyester and polyethylene geogrids was increased by cyclic loading and also increased by load ratio. The stiffness of these geogrids increased following cycles of loading, especially at high load ratios. A hyperbolic relationship was suggested to express the strain induced by cyclic loading of the geogrids.

The results for PET and HDPE followed the trend reported by Bathurst and Cai (1992) and Moraci and Montanelli (1996, 1997). Generally speaking, the tensile properties of three types

of geogrids were not degraded significantly due to short-term cyclic loading. The current practice of using the results from static tests for seismic design appears reasonable. The good performance of geosynthetic-reinforced soil structures during recent earthquakes could possibly be due to the reinforcement acting satisfactorily as energy absorber (i.e., due to its damping properties). The details of tensile behavior, incorporating stiffness and damping properties, should be investigated by employing a more sophisticated numerical tool with robust constitutive models for geogrid and soil.

Generalization of these results to other types of geogrid should be confirmed by additional testing.

## APPENDIX. REFERENCES

- Ashwamy, A. K., and Bourdeau, P. L. (1996). "Response of a woven and a nonwoven geotextile to monotonic and cyclic simple tension." *Geosynthetics Int.*, 3(4), 493–515.
- Bathurst, R. J., and Cai, Z. (1994). "In-isolation cyclic load-extension behavior of two geogrids." *Geosynthetics Int.*, 1(1), 1–19.
- Koerner, R. M. (1998). *Designing with geosynthetics*, 4th Ed. Prentice Hall, Englewood Cliffs, N.J.
- Moraci, N., and Montanelli, F. (1996). "Short and long term behavior of geogrids under static and cyclic load." *Earth reinforcement*, Ochiai et al., eds., Balkema, Rotterdam, The Netherlands, 117–122.
- Moraci, N., and Montanelli, F. (1997). "Behavior of geogrids under cyclic loads." *Proc., Geosynthetic '97 Conf.*, 961–976.